Game theory and the evolution of cancer

Bernat Ramis
supervised by Tobias Galla
Instituto de Física Interdisciplinar y Sistemas Complejos, IFISC (CSIC-UIB)
Campus Universitat de les Illes Balears, E-07122 Palma de Mallorca, Spain

Abstract

This project aims to use evolutionary game theory to develop a model based on Moran processes for two different kinds of individuals competing for reproduction and survival. Our model takes into account the different fitnesses of species, mutation and ageing. We implemented the model with stochastic simulations in order to draw conclusions. As an application, it can model the evolution of a community of cancer cells.

1 Introduction

This introduction to evolutionary game theory is inspired by [1].

1.1 Game theory: Prisoner's dilemma and its variations

In game theory, one studies situations involving a number of individuals whose decisions or strategies affect the whole community. The canonical example is the *prisoner's dilemma*.

Concerning our interest, imagine a system consisting of two kinds of individuals that interact (e.g. for survival or reproduction). So-called A individuals adopt a certain strategy while B individuals behave according to other rules. This interaction may be modeled using "rewards" or "costs", which depend on which strategies encounter. For two different strategies, we have four possible situations, as depicted in Tab. 1.

	A	**B**
A	R	S
B	T	P

Table 1: Payoff matrix. R, S, T and P (standing for Reward, Sucker's payoff, Temptation and Punishment, respectively, as in the *prisoner's dilemma*) represent real positive numbers, which are the payoffs for the player on the leftmost column when an encounter of strategies takes place. The uppermost row collects the possible strategies of the opponent. For instance, a B individual battling against an A individual would be rewarded an amount of T.

Here, the concept of Nash equilibrium arises.

Definition 1.1. A set of strategies for some given players is called to be a **Nash equilibrium** if any change in the strategy of any player would not improve their chances of beating the others. These configurations fully depend on the values of R, S, T and P.

1.2 First-order ODE approach

Definition 1.2. According to Tab. 1, the **fitness** of a given strategy (say strategy A) is defined as follows:

$$\pi_A(a) := 1 + \mathrm{R}a + \mathrm{S}b = 1 + \mathrm{R}a + \mathrm{S}(1-a) \tag{1}$$

where $a := N_A/N$ is the fraction of individuals of kind A present in the whole population considered. Here, we used that only two strategies are possible (A and B), thus $b = 1 - a$.

Observation 1.1. The additive term 1 present in the formula is the background fitness, and it is mainly added so that the fitness is strictly positive, which is required in later definitions. The remaining terms are the average payoff expected when playing the game (performing strategy A, in the case considered in Eq. (1)).

Definition 1.3. Average fitness:

$$\overline{\pi}(a) := a\pi_A(a) + b\pi_B(b) = a\pi_A(a) + (1-a)\pi_B(a) \tag{2}$$

This magnitude is useful to measure the mean gain of an individual in a community where different strategies coexist.

We finally get to the first-order ODEs.

Definition 1.4. Standard replicator equation

$$\partial_t a = [\pi_A(a) - \overline{\pi}(a)]a \tag{3}$$

Definition 1.5. Adjusted replicator equation

$$\partial_t a = \frac{\pi_A(a) - \overline{\pi}(a)}{\overline{\pi}(a)}\, a \tag{4}$$

Both of the above presented equations tell that the population of A individuals will grow proportionally to the actual amount of A individuals and proportionally to the difference between the fitness of A and the mean fitness. Notice that if the fitness of A is larger than the mean fitness, then the population of A will increase (since, in average, they tend to win more often). Likewise, if the fitness of A is lower than the mean fitness, the population of A will decrease. The previous equations can analogously describe the evolution of the fraction of individuals of other strategies (strategy B with a fraction of individuals b).

Eq. (3) can be rewritten as

$$\partial_t a = a(1-a)[\mu_A(1-a) + \mu_B a] =: F(a) \tag{5}$$

where $\mu_A := \mathrm{S} - \mathrm{P}$ and $\mu_B := \mathrm{T} - \mathrm{R}$ are the relative benefits of A playing against B and B playing against A, respectively. Now the relative payoff matrix looks like in Tab. 2.

	A	**B**
A	0	μ_A
B	μ_B	0

Table 2: Relative payoff matrix. Only relative payoffs are relevant (difference of gains for each encounter).

The values of the control parameters μ_A and μ_B make possible a classification into four kinds of games:

Game	control parameters	stable fixed points
Prisoner's dilemma	$\mu_A < 0$ $\mu_B > 0$	$a = 0$
Snowdrift/Coexistence	$\mu_A > 0$ $\mu_B > 0$	$a = \frac{\mu_A}{\mu_A + \mu_B}$
Coordination	$\mu_A < 0$ $\mu_B < 0$	$a = 0,\ 1$
Harmony	$\mu_A > 0$ $\mu_B < 0$	$a = 1$

Table 3: Game classification using the criterion of the relative benefits μ_A and μ_B. For the fixed points, recall that it is needed that $F(a) = 0$ in Eq. (5). Moreover, for a fixed point to be stable, it is sufficient that $F'(a) < 0$, because if $F(a) = 0$ then $F(a+h) < 0$ for small $h > 0$ so this means that $\partial_t a < 0$ and thus $a + h$ decreases to a, meaning there is an attraction towards a (attraction is also concluded assuming $h < 0$). Accordingly, stable fixed points for each set of control parameters can be analytically derived. The names of the games describe the location of the stable fixed points. For example, in a Coordination game, stability arises when all players in the community carry out the same strategy (either A or B).

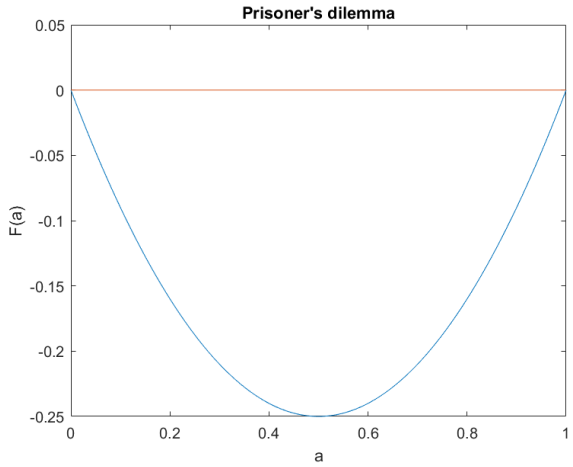

(a) $\mu_A = -1, \mu_B = -1$.

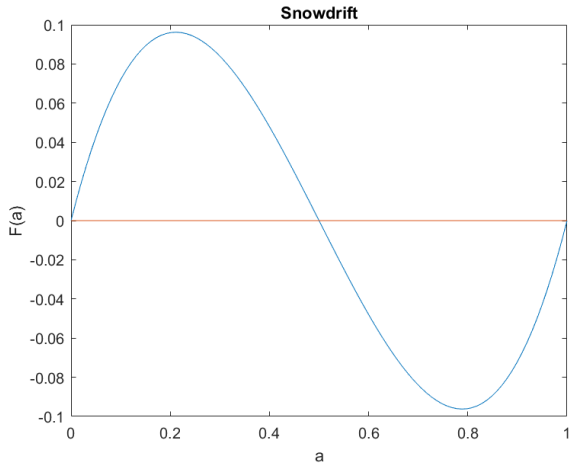

(b) $\mu_A = 1, \mu_B = 1$.

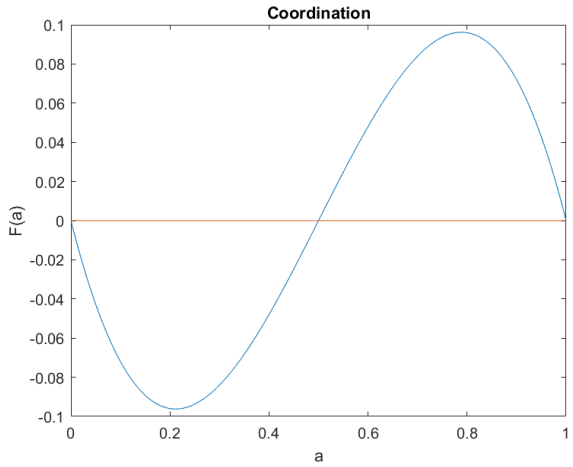

(c) $\mu_A = -1, \mu_B = -1$.

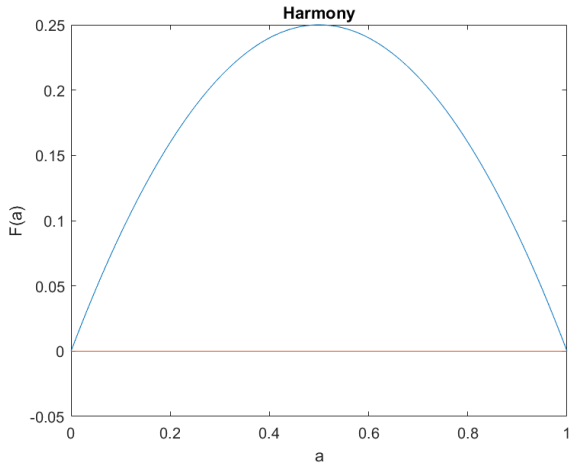

(d) $\mu_A = 1, \mu_B = -1$.

Figure 1: Plots of $F(a)$ in Eq. (5) split by different cases for different control parameters μ_A and μ_B. Stable fixed points can be found identifying the values of a such that $F(a) = 0$ and $F'(a) < 0$. Points for which $F(a) = 0$ and $F'(a) > 0$ are unstable fixed points.

For the fixed points, recall that it is needed that $F(a) = 0$ in Eq. (5). Moreover, for a fixed point to be stable, it is sufficient that $F'(a) < 0$, because if $F(a) = 0$ then $F(a + h) < 0$ for small $h > 0$ so this means that $\partial_t a < 0$ and thus $a + h$ decreases to a, meaning there is an attraction towards a (attraction is also concluded assuming $h < 0$).

The plots in Fig. 1 are perfectly coherent with the above classification: one can detect a stable fixed point in a plot by identifying the points where $F(a) = 0$ and $F'(a) < 0$. In this case, it is often referred to as Nash equilibrium points. Besides, points such that $F(a) = 0$ and $F'(a) > 0$ are unstable fixed points.

We would like this theory about the payoff matrix to underlie the model that we develop for confrontation between two different strategies.

2 Individual based model

2.1 Moran processes

Consider two kinds of individuals, A and B. We use N_A and N_B to denote the number of individuals of the type they are labelled.

Definition 2.1. A **Moran process** is a stochastic process for modelling populations of a finite number of individuals, each belonging to type A or B. To carry the process out, at each time step two individuals are chosen at random among the available population. Then, according to certain probabilities, which depend on the fitnesses of the selected individuals, maybe one of them is chosen

to die and the remaining one replicates, or maybe nothing happens. Overall, if we focus just on the number of individuals of each type, one of the following transitions may occur at each time step:

- $(N_A, N_B) \to (N_A + 1, N_B - 1)$
- $(N_A, N_B) \to (N_A - 1, N_B + 1)$
- $(N_A, N_B) \to (N_A, N_B)$

Observe that $N_A + N_B = N$ is constant during the process. It is useful to introduce a variable i that counts the number of A individuals N_A present in the system at any time, as in Fig. 2. T_i^+ and T_i^- denote the probabilities of transition of number of A individuals. Also take into account that these probabilities for each transition at each time step can be different (usually, these probabilities depend on i).

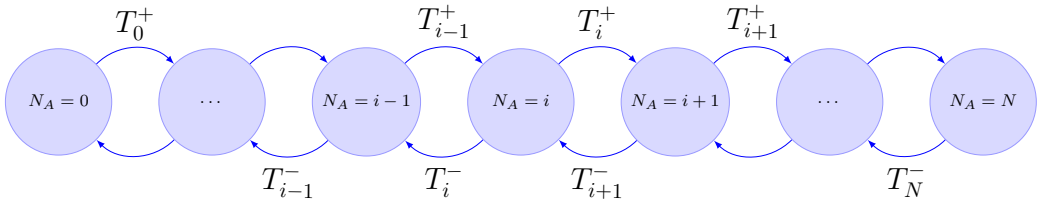

Figure 2: Diagram of a Moran process. At each time step, the i variable (which takes the value of the number of A individuals present in the community in that moment) may increase or decrease its value by 1, meaning that a new A individual replaced a B individual or vice versa. The probabilities for this to happen, which depend precisely on i, are denoted as T_i^+ for increasing i transitions and T_i^- for decreasing i transitions. It always holds that $T_i^+ + T_i^- \leq 1$ for $i = 1, \ldots, N$.

In Moran processes, fixation times are an interesting magnitude to study.

Definition 2.2. Unconditional fixation time: expected time elapsed starting with 1 individual of kind A and ending up with only one kind of individuals (either A or B).

Definition 2.3. Conditional fixation time (for A individuals): expected time elapsed starting with 1 individual of kind A and ending up with only A individuals.

Fixation time analytical expressions may be derived from recurrences, see [2]. In an attempt to study them with simulations, the results look like in Fig. 3.

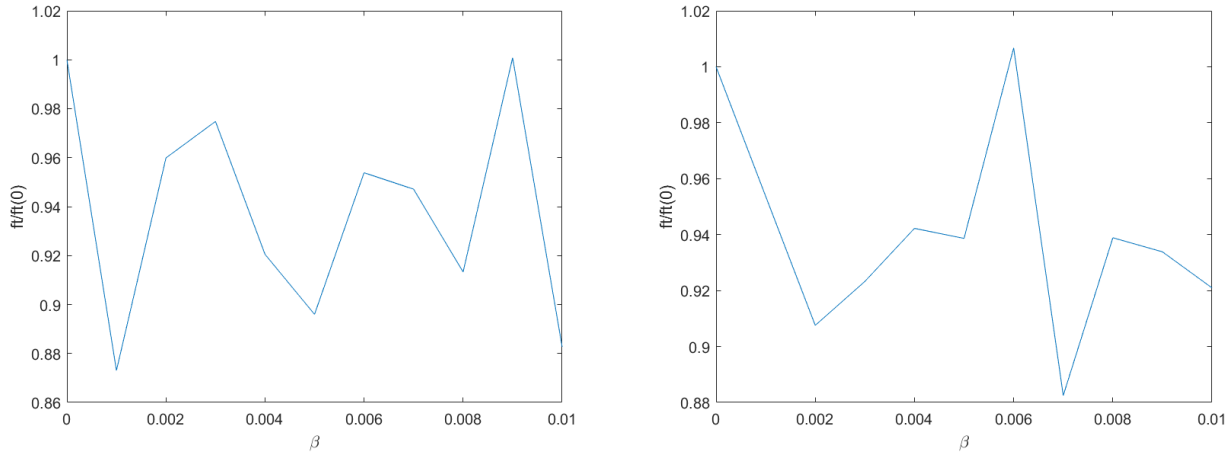

(a) Unconditional fixation time

(b) Conditional fixation time

Figure 3: Relative fixation time $\frac{\text{fixation time}(\beta)}{\text{fixation time}(\beta=0)}$ as a function of the fitness importance parameter β. Parameters chosen are $N = 10$, $M = \begin{pmatrix} 5 & 2 \\ 3 & 1 \end{pmatrix}$ and initially $N_A = 1$. Only 500 samples for each averaged β value. Since the variance of the fixation time is huge, we get nothing close to linear plots.

Theory says that for small β, one can get decent linear approximations for fixation times as a function of β. However, this is not what Fig. 3 depicts. In order to fix this issue, we need a set of

the order of 10^7 samples to reduce the effect of the variance in fixation times, which is large. For less samples, the results are more like in Fig. 3.

As Fig. 4 and Fig. 5 show, outputs from simulations follow the theoretical results obtained in [2].

At least for $0 < \beta < 0.01$ the linear approximation is valid. Observe that according to the M payoff matrices, Fig. 4 stems from a drag game whereas Fig. 5 comes form a coordination game.

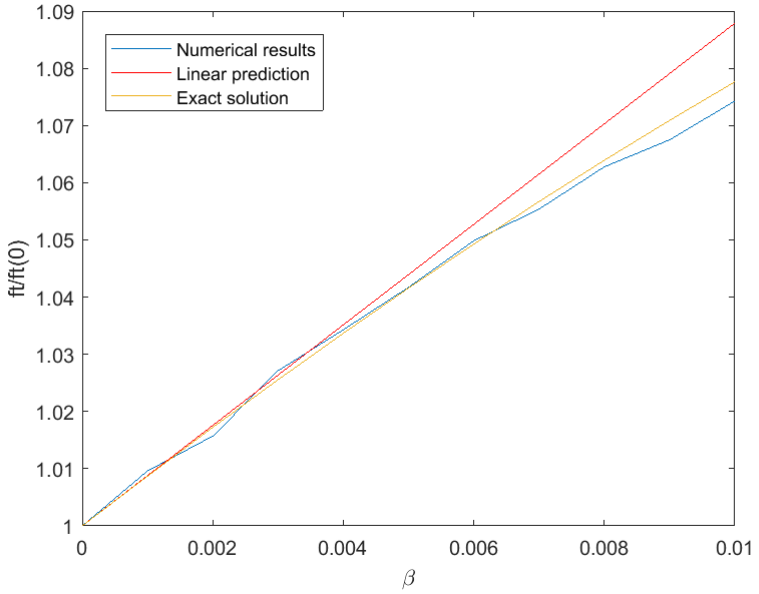

Figure 4: Relative unconditional fixation time $\frac{\text{fixation time}(\beta)}{\text{fixation time}(\beta=0)}$ as a function of the fitness importance parameter β (see Eq. (15)). Parameters chosen are $N = 100, M = \begin{pmatrix} 5 & 2 \\ 3 & 1 \end{pmatrix}$ and initially $N_A = 1$. 10^7 samples taken. Now the averaged fixation times obtained from simulations do follow the theoretical results, as well as they both graze the linear prediction.

2.2 Evolutionary games with ageing

We will now consider a population of agents interacting in an evolutionary game, but subject to ageing. By this we mean a setup in which the success or otherwise of an agent depends on their "age", that is the time since they were born.

To this end we consider a population of N agents, who can each be of type A or type B. We write N_A for the number of agents of type A, the number of agents of type B is then $N - N_A$. Each of the agents has an age τ_i, where $i = 1, \ldots, N$ labels the agents.

We choose a discrete-time setup for convenience (but can also generalise to continuous time later). The model proceeds as follows:

1. Time $t = 0$. Initialise the population. All agents have age zero ($\tau_i \equiv 0 \; \forall i$). The initial number of agents of type A is set to $N_A = N_{A,0}$.
2. At each step of the simulation pick two distinct agents i and j ($i \neq j$). Let $\pi^{(i)}$ and $\pi^{(j)}$ be their fitnesses. $\pi^{(i)}$ will only depend on what type agent i is of (A or B) and on the composition of the population, i.e. the number N_A of agents of type A. For example, if i is of type A, then $\pi^{(i)} = \pi_A(N_A)$.
3. We now need to decide if agent i reproduces (and j dies) or vice versa. We do this with the following probabilities:

$$\begin{aligned} &i \text{ reproduces with probability } p_i = g(\pi_i - \pi_j) \times h(\tau_i, \tau_j), \\ &j \text{ reproduces with probability } p_j = g(\pi_j - \pi_i) \times h(\tau_j, \tau_i). \end{aligned} \tag{6}$$

4. Once decided what agent reproduces (if any does), kill the other one. The reproducing agent reproduces. With probability $1 - \mu$ the offspring will be of the same type (A or B) as

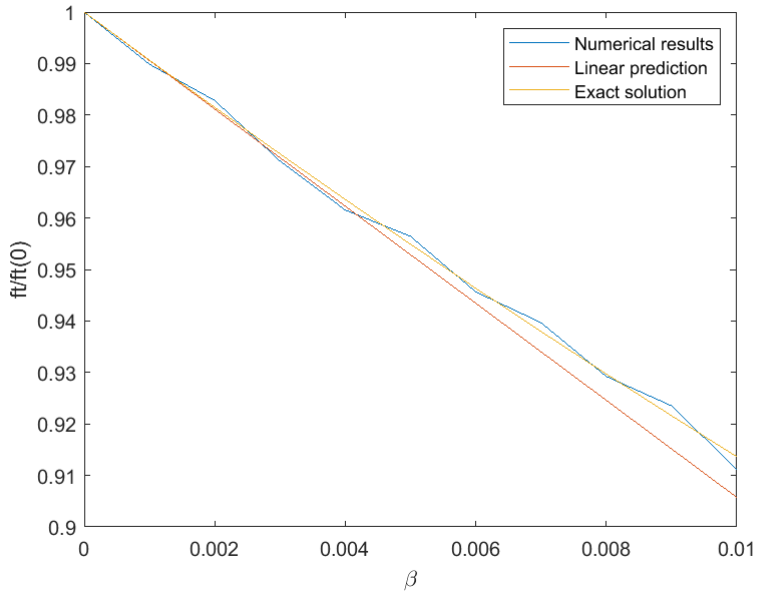

Figure 5: Relative unconditional fixation time $\frac{\text{fixation time}(\beta)}{\text{fixation time}(\beta=0)}$ as a function of the fitness importance parameter β. Parameters chosen are $N = 100, M = \begin{pmatrix} 5 & 1 \\ 3 & 2 \end{pmatrix}$ and initially $N_A = 1$. 10^7 samples taken. Once again, numerical results agree with theoretical expressions.

the reproducing agent, i.e., no mutation occurs. With probability μ a mutation occurs, the offspring is of the opposite type as the parent. The age of the offspring is set to zero.

5. The ages of all agents increase by Δt (the length of the time step), and overall time is also incremented by Δt. Then go to step 2.

Choice of time step:
The natural choice for the time step is $\Delta t = 1/N$. This means that order N events happen per unit time, so each agent is picked order one times per unit time.

Further remarks:

- The function $g(\cdot)$ describes selection based on fitness difference. This could be chosen as the Fermi function
$$g(\Delta\pi) = \frac{1}{1 + e^{-\beta\Delta\pi}}, \tag{7}$$
but other choices are possible as well. Note that $g(\cdot)$ needs to be an increasing function of $\Delta\pi$. The parameter β characterises the intensity of selection.
- We also need to decide how the ages of the agents affect the process. This is what the function $h(\cdot,\cdot)$ does. There are several simple choices:
  - Age only affects the probability to reproduce, $h(\tau_i, \tau_j) = h(\tau_i)$.
  - Age only affects the probability to die, $h(\tau_i, \tau_j) = h(\tau_j)$.
  - Only age difference matters, $h(\tau_i, \tau_j) = h(\tau_i - \tau_j)$.

  In each of these cases the resulting function $h(x)$ can be increasing or decreasing (depending on whether young individuals should have advantage over old ones or the other way around) and could take different shapes (e.g. exponential, power law, etc.).

2.3 Comparison of fixation times

In order to study how ageing affects fixation times compared with the lack of ageing case, it would not be fair to multiply the probability to reproduce $g(\cdot)$ by the new ageing probability function $h(\cdot)$, because in such a case the probability for nothing to happen would be increased and thus the process slows down, in the sense that more rounds without anything happening occur.

If an A individual meets a B individual, let p^+ be the probability that the A participant replicates substituting the B one, and let p^- be the vice versa probability. Coherently, $p^+ + p^- \leq 1$. An

alternative we propose is defining two coefficients $\alpha = \alpha(\tau)$ and $\beta = \beta(\tau)$ that reward or punish the probabilities p^+ and p^- according to the age of the fighters chosen, keeping the probability for nothing to happen unchanged:

$$\begin{aligned} p^+ + p^- &=: s \\ \alpha p^+ + \beta p^- &= s \end{aligned} \tag{8}$$

Now defining the ratio $r := \frac{\alpha}{\beta}$ and manipulating Eq. (8),

$$r = \frac{\alpha}{\beta} = \frac{\frac{s}{\beta} - p^-}{p^+} \implies \beta = \frac{s}{rp^+ + p^-}. \tag{9}$$

At this point, we may choose the ratio r. Then, α and β become uniquely determined. Here, although many possibilities arise, we wish that:

- $r \in \left[\frac{1}{2}, 2\right]$ so that the weights α and β are not extremely unbalanced.
- r should depend on the age of the pair of individuals considered. Let $r\left(\frac{\tau_i}{\tau_j}\right)$ depend on the ratio of ages, $R := \frac{\tau_i}{\tau_j}$.
- It is reasonable to ask that $r\left(\frac{1}{R}\right) = \frac{1}{r(R)}$, for all R. This way, r (or $\frac{1}{r}$) does not depend on the order of the ages of the pair of individuals (up to inverse).
- Consequently, it is natural to require that $r(1) = 1$ and $r(0) = \frac{1}{2} \equiv r(\infty) = 2$.

Observation 2.1. Functions of the kind

$$r(R) = \frac{\sum_{i=0}^{k} d_i R^i}{\sum_{i=0}^{k} d_{k-i} R^i} \tag{10}$$

with $k \in \mathbb{N}$ and $d_i \in \mathbb{R}$ for $i = 1, \ldots, k$, solve the functional equation $r\left(\frac{1}{R}\right) = \frac{1}{r(R)}$.

For simplicity, we choose

$$r(R) = \frac{AR + B}{BR + A} = \frac{R + \gamma}{\gamma R + 1} \tag{11}$$

with $\gamma := \frac{B}{A}$, which is determined imposing the point conditions. It is already fulfilled that $r(1) = 1$. Now, $r(0) = \gamma = \frac{1}{2}$, so we end up with

$$r(R) = \frac{2R + 1}{R + 2}. \tag{12}$$

Observation 2.2. The greater N, the greater the lifetimes τ_i of the individuals tend to be. However, since the ratios $R := \frac{\tau_i}{\tau_j}$ are the variables, it is not needed to take into account an N dependency in the function $r(R)$.

To sum up, including ageing in the model the way proposed implies updating the probabilities p^+ and p^- as follows:

- $p^+ \to \alpha p^+$
- $p^- \to \beta p^-$

where $r(R)$ is Eq. (12), β is Eq. (9) and $\alpha = r(R)\beta$.

2.4 Deterministic equations

We derive equations for the designed model, inspired by [3].

- x: fraction of A individuals
- x_i^+: fraction of A individuals and age i
- x_i^-: fraction of B individuals and age i
- $p_d^+(i)$: probability that an A individual of age i dies
- $p_d^-(i)$: probability that a B individual of age i dies
- $s^{-\to+}(i)$: probability to switch from B and age i to A and age 0 (without mutating)
- $s^{+\to-}(i)$: probability to switch from A and age i to B and age 0 (without mutating)

$$\begin{cases} \frac{dx_i^+}{dt} = -x_i^+ + x_{i-1}^+(1 - p_d^+(i-1)) \\ \frac{dx_i^-}{dt} = -x_i^- + x_{i-1}^-(1 - p_d^-(i-1)) \\ \frac{dx}{dt} = \sum_{i=0}^{\infty} x_i^- s^{-\to+}(i) - \sum_{i=0}^{\infty} x_i^+ s^{+\to-}(i) \end{cases} \tag{13}$$

To include ageing in the infinite system of equations, it is required to take ageing into account in $p_d^+(i)$, $p_d^-(i)$, $s^{-\to+}(i)$ and $s^{+\to-}(i)$, as follows.

$$\begin{aligned} p_d^{\pm}(i) &= \frac{\sum_j p_d(i|\text{opponent's age is } j) x_j^{\pm}}{\sum_j x_j^{\pm}} \\ s^{-\to+}(i) &= p_d^-(i)(1-\mu) \\ s^{+\to-}(i) &= p_d^+(i)(1-\mu) \end{aligned} \tag{14}$$

μ is the probability of mutation.

3 Results and discussion from simulations

3.1 Lifetime distribution for Moran processes

Now the question to be answered is, in an ageingless Moran process, what does the distribution of individual lifetimes look like? To dive into the context, imagine a population of individuals of kinds A and B, together with a certain payoff matrix M that induces a set of probabilities for the individuals to die or reproduce. If one focuses on a specific individual, say of kind A, how long is it expected to live and what is the probability distribution behind?

Hereinafter, the choices for the setup are the following.

- Consider the distribution of deaths for a kind A individual.
- Fermi distribution of probability of death for direct encounters:

$$p_-(\Delta\pi) = \frac{1}{1 + e^{-\beta\Delta\pi}}. \tag{15}$$

- Coexistence payoff matrix, in particular $M = \begin{pmatrix} 3 & 2 \\ 5 & 1 \end{pmatrix}$.
- Probability of mutation of 5%. Mutation will prevent the system from fixation.
- Initial conditions with one only individual of kind A.
- The number of individuals N and the parameter β remain free for later exploration.
- Lifetime is computed as the number of rounds that an individual survives since it was born.

We now compute of the probability that a given individual dies. Firstly, the individual has to be chosen, event that takes place with probability $1/N$. Afterwards, the second competitor can either be of kind A or B. An A would be picked with probability $\frac{i-1}{N-1}$. If two A's compete, the probability of losing is 0.5 according to the Fermi distribution, Eq. (15).

If instead of being A, the second individual were B, which would happen with probability $\frac{N-i}{N-1}$, then the given individual would die with probability $p^-(i)$.

Finally, since the pair of individuals can be chosen in two different orders, a factor 2 is introduced, leading to

$$p_d(i) := p_{death}(i) = \frac{1}{N(N-1)}(i - 1 + 2(N-i)p_-(i)). \tag{16}$$

Imagine for a moment that $p_d(i)$ was constant on the number of A individuals i. Then, the distribution for the lifetime random variable LT would be geometric of parameter p_d, $LT \sim \text{Geom}(p_d)$, i.e.

$$p(LT = t) = (1 - p_d)^t p_d, \quad t = 0, 1, 2, \ldots \tag{17}$$

where t is the number of rounds survived.

In general, $p_d(i)$ will not be constant, so in principle Eq. (17) does not necessarily work. It will if the fluctuations of $p_d(i)$ with time are little, although for large fluctuations the distribution may be deformed to an extend that it is no longer geometric. The work now is to study this by varying β and N in the simulations. As a start, let $N = 100$ and focus on the order of magnitude of β.

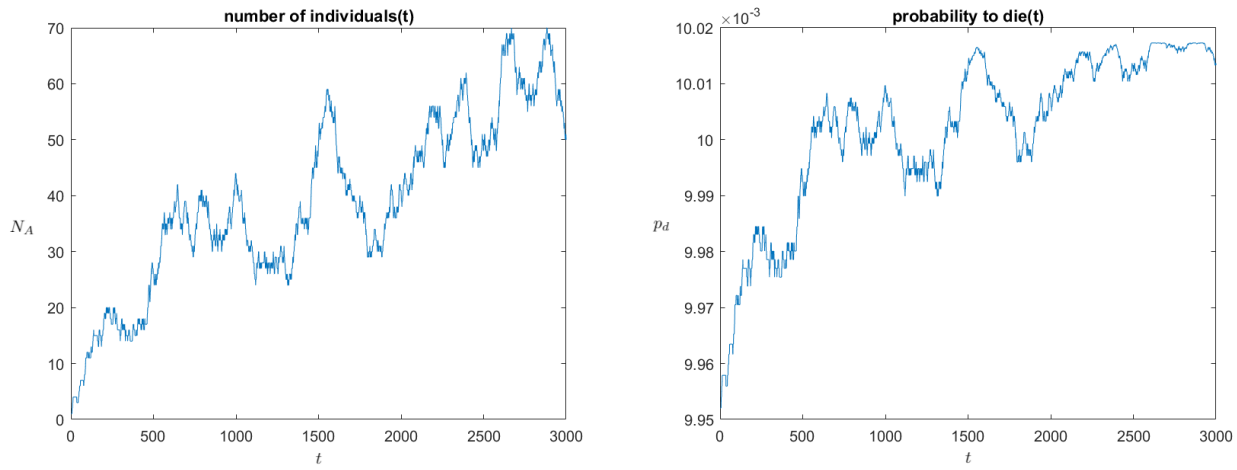

(a) (b)

Figure 6: Number of A individuals N_A and probability of an A individual to die p_d as a function of time t, from a stochastic simulation with parameters $N = 100$, $N_{A,0} = 1$, 10^5 lifetime samples taken, probability of mutation $\mu = 5\%$, $M = \begin{pmatrix} 3 & 2 \\ 5 & 1 \end{pmatrix}$ and $\beta = 0.01$. Both magnitudes tend to oscillate around their equilibrium values, given by the equilibrium N_A, which at the same time is determined by the payoff matrix M. This is a case of so-called weak selection, since the value of β is small. Consequently, oscillations around equilibrium values are larger than for stronger selection.

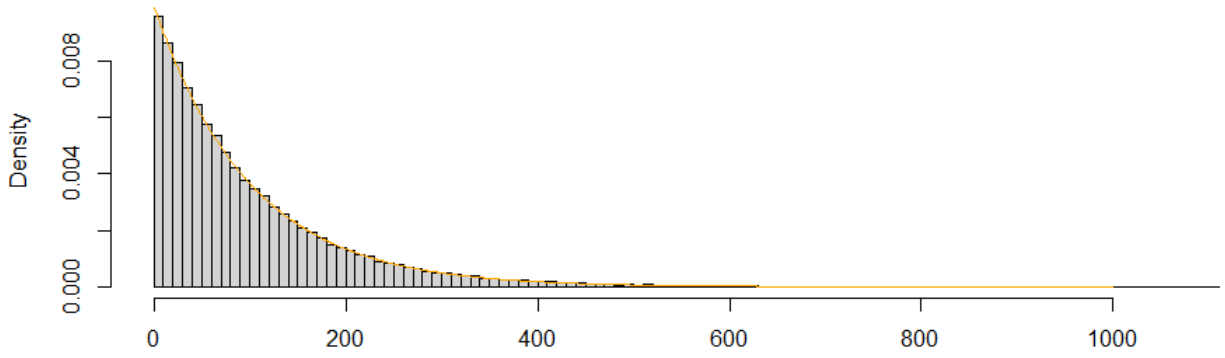

Figure 7: In grey, the normalised histogram or empiric probability density function of the simulation that yielded Fig. 6. In orange, the theoretical shape of a Geom(1/100)=Geom($1/N$) distribution. We observe coincidence.

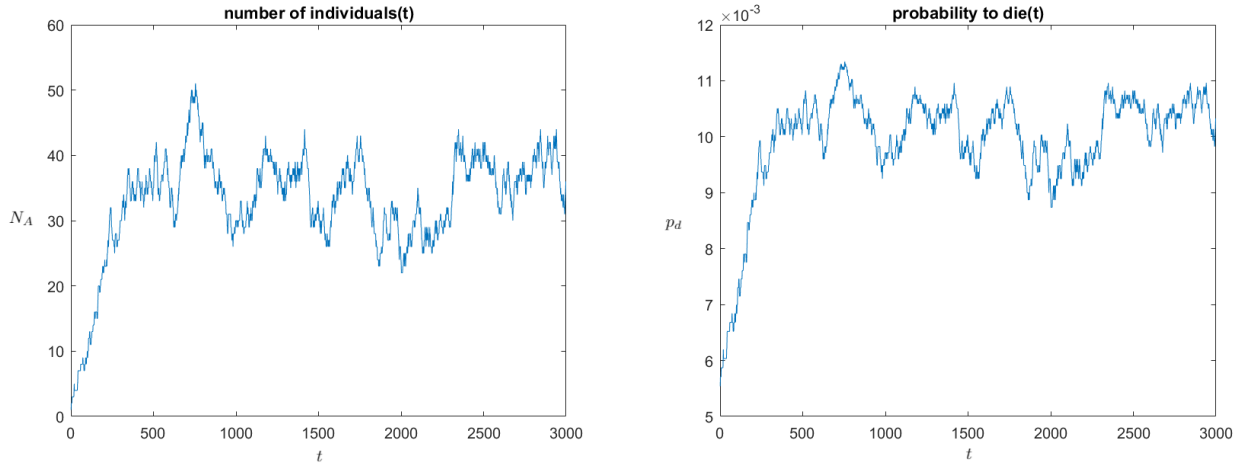

(a) (b)

Figure 8: Number of A individuals N_A and probability of an A individual to die p_d as a function of time t, from a stochastic simulation with parameters $N = 100$, $N_{A,0} = 1$, 10^5 lifetime samples taken, probability of mutation $\mu = 5\%$, $M = \begin{pmatrix} 3 & 2 \\ 5 & 1 \end{pmatrix}$ and $\beta = 1$. Both magnitudes tend to oscillate around their equilibrium values, given by the equilibrium N_A, which at the same time is determined by the payoff matrix M. Oscillations are weaker than those in Fig. 6 due to a larger β.

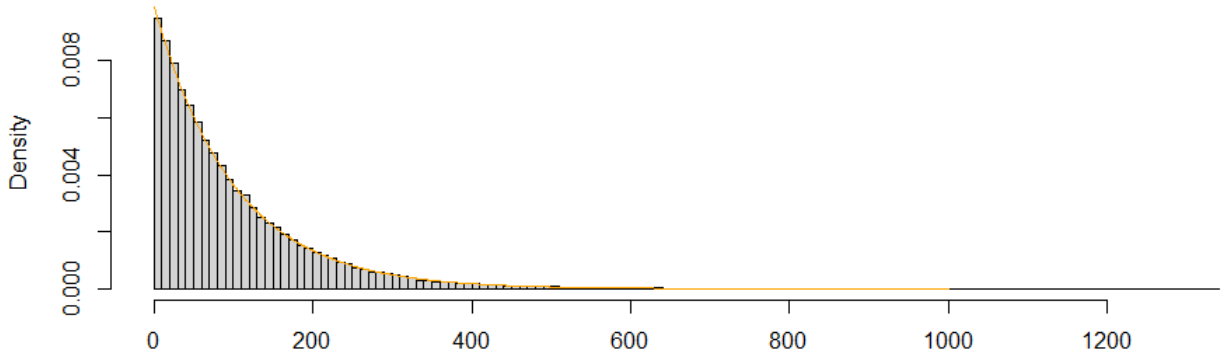

Figure 9: In grey, the normalised histogram or empiric probability density function of the simulation that yielded Fig. 8. In orange, the theoretical shape of a Geom(1/100)=Geom($1/N$) distribution. We observe coincidence.

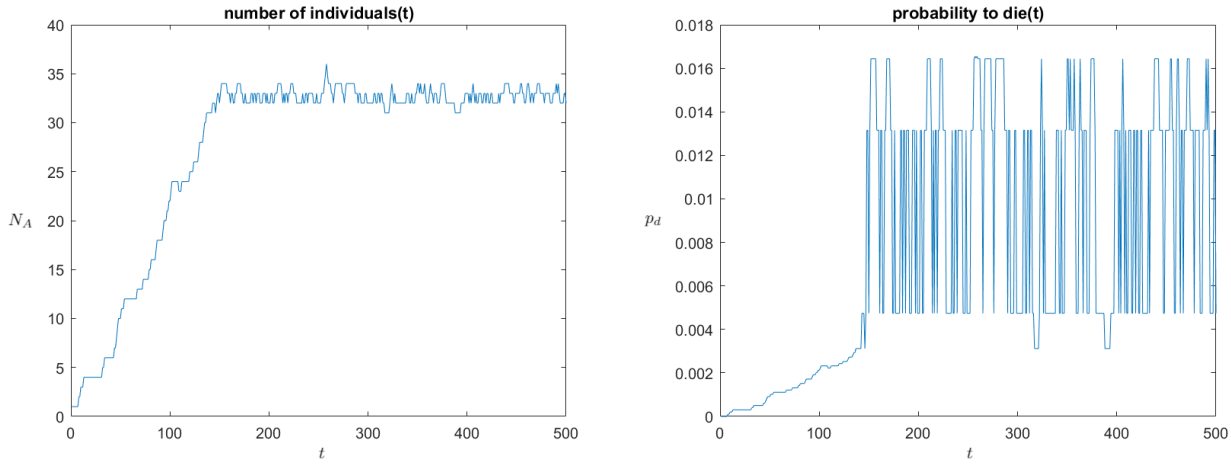

(a) (b)

Figure 10: Number of A individuals N_A and probability of an A individual to die p_d as a function of time t, from a stochastic simulation with parameters $N = 100$, $N_{A,0} = 1$, 10^5 lifetime samples taken, probability of mutation $\mu = 5\%$, $M = \begin{pmatrix} 3 & 2 \\ 5 & 1 \end{pmatrix}$ and $\beta = 100$. Both magnitudes tend to oscillate around their equilibrium values, given by the equilibrium N_A, which at the same time is determined by the payoff matrix M. A large value for β, like in this case, yields tight oscillations.

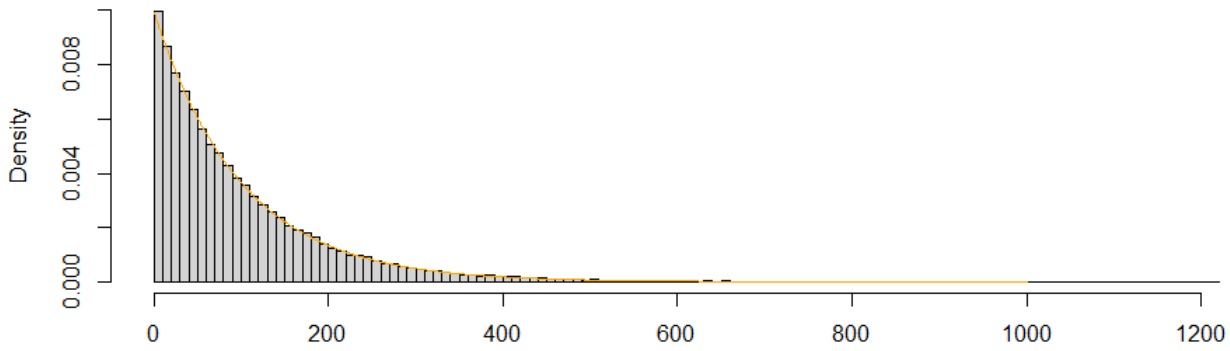

Figure 11: In grey, the normalised histogram or empiric probability density function of the simulation that yielded Fig. 10. In orange, the theoretical shape of a Geom(1/100)=Geom(1/N) distribution. We observe coincidence.

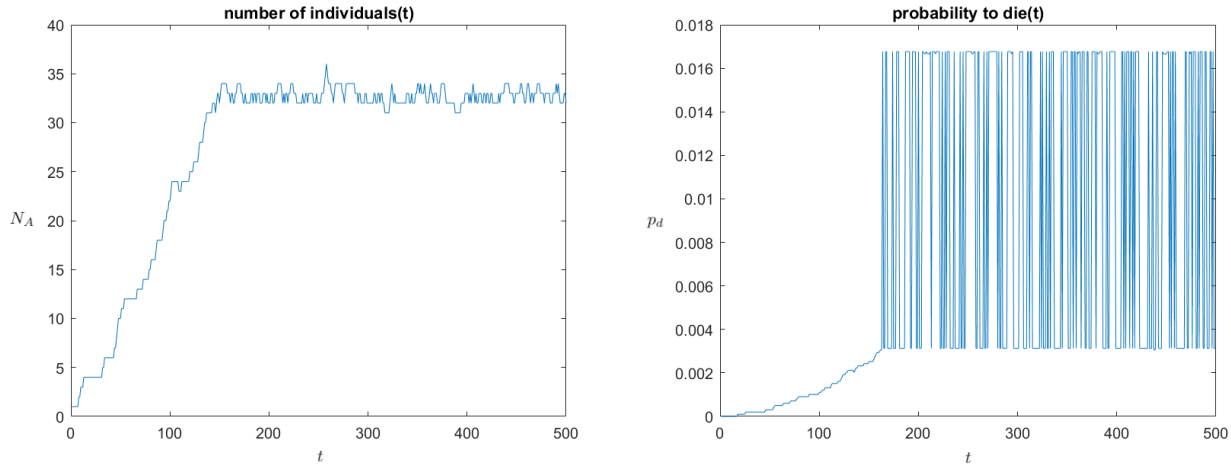

(a) (b)

Figure 12: Number of A individuals N_A and probability of an A individual to die p_d as a function of time t, from a stochastic simulation with parameters $N = 100$, $N_{A,0} = 1$, 10^5 lifetime samples taken, probability of mutation $\mu = 5\%$, $M = \begin{pmatrix} 3 & 2 \\ 5 & 1 \end{pmatrix}$ and $\beta = 10000$. Both magnitudes tend to oscillate around their equilibrium values, given by the equilibrium N_A, which at the same time is determined by the payoff matrix M. The value for β used is even unrealistic, but we try to see if the lifetime distribution is deformed when the range of frequent values of N_A is smaller that 5 values. Fig. 13 shows that this is not the case.

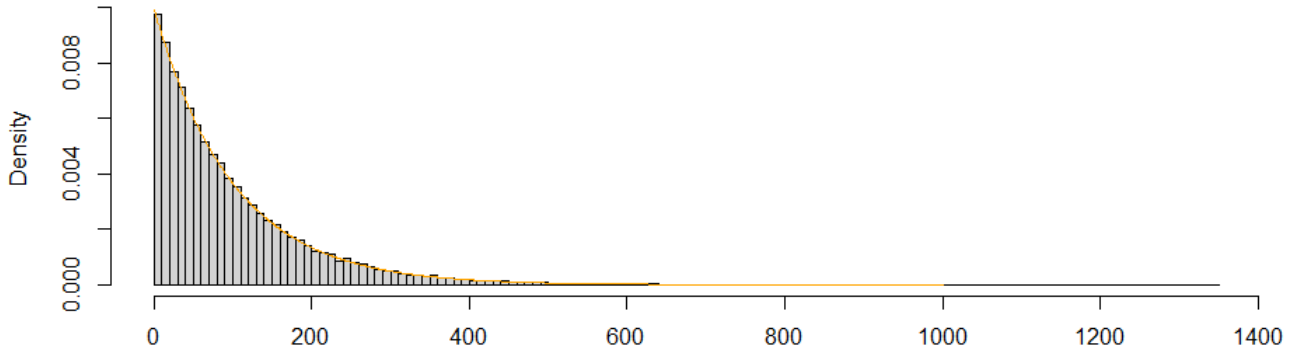

Figure 13: In grey, the normalised histogram or empiric probability density function of the simulation that yielded Fig. 12. In orange, the theoretical shape of a Geom(1/100)=Geom(1/N) distribution. We observe coincidence.

It is concluded that for $N = 100$, even though β varies, the empiric density functions are fitted by the orange theoretical geometrical with parameter $1/N = 1/100$ density function. Introducing logarithms in Eq. (17),

$$\log(p_d(i)) = t\log(1 - p_d) + log(p_d) \tag{18}$$

so $[\log(p_d)](t)$ should be a linear dependency under the hypothesis that p_d can be considered constant. It turns out to be true for $N = 100$, Fig. 14.

Recall the fixed point of the coexistence/snowdrift game in Tab. 3, that for this particular case ($N = 100$ and $\beta = 1$) is position $N\frac{\mu_A}{\mu_A+\mu_B} \simeq 33$, for which $p_d(33) = 0.0100342 \simeq 0.01 = 1/100$. The conclusion is that fluctuations were not strong enough to disrupt the distribution. This causes no surprise after checking the probability values around the stable position in Tab. 4.

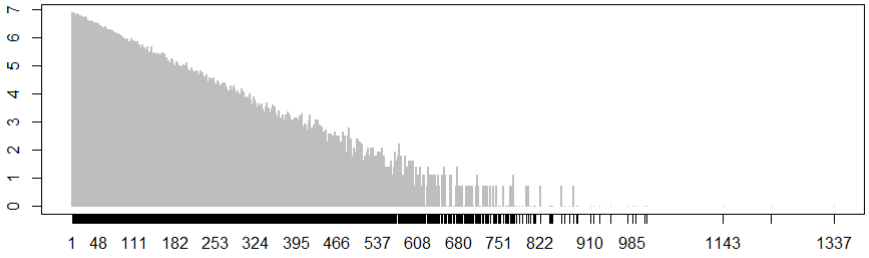

Figure 14: Plot of the logarithm of histogram in Fig. 9. Corroboration of linearity that confirms a distribution Geom(1/100) for $N = 100$ and $\beta = 1$, so with the setting that yielded Fig. 8 and Fig. 9. Noise for large lifetimes is due to the finite run time of the simulation, which does not let all potential "long livers" die (the simulation stops when the desired number of lifetime samples is reached).

To get a feeling of how much the magnitude of the fluctuations of p_d deforms the geometric distribution, we made a short script in *R*. It created 100000/2 Geom(0.01+ϵ) samples and other 100000/2 Geom(0.01-ϵ) samples (since the simulation produced 100000 samples). Applying the statistical t-test to check whether the mean of the distribution behind the samples was $p = 0.01$, the smallest order of magnitude of ϵ for the mean not to be the corresponding $\frac{1}{p}-1$ (with significance value $\alpha = 0.05$) was $\epsilon = 0.0009$ (thus $\Delta\epsilon = 0.0018$), which is greater that the fluctuations in Tab. 4. As a consequence, the fluctuations did not modify the mean of the distribution of lifetimes.

position i	p_d
27	0.00936845
28	0.00948662
29	0.00960198
30	0.00971447
31	0.00982403
32	0.00993062
33	0.0100342
34	0.0101347
35	0.010232
36	0.0103262
37	0.0104172
38	0.010505
39	0.0105895

Table 4: Probabilities p_d around equilibrium position 33, in the setting of simulations that leaded to Fig. 8. The order of magnitude of the fluctuations (10^{-4}) was not big enough to disrupt the geometrical distribution.

Essentially, the parameter p_d does not significantly change. The same happens for small values of β (neutral/weak selection) and for large ones (strong selection), as seen in Fig. 6 - Fig. 13. Having a look back at Eq. (16), since there appears a strong factor $\frac{1}{N(N-1)}$, to get larger fluctuations it is probably required small N to obtain stronger fluctuations that may break the geometrical distribution.

However, it turns out that for small N, the resulting distribution is still geometric, as Fig. 15 shows, even though probabilities in Tab. 5 fluctuate stronger than before.

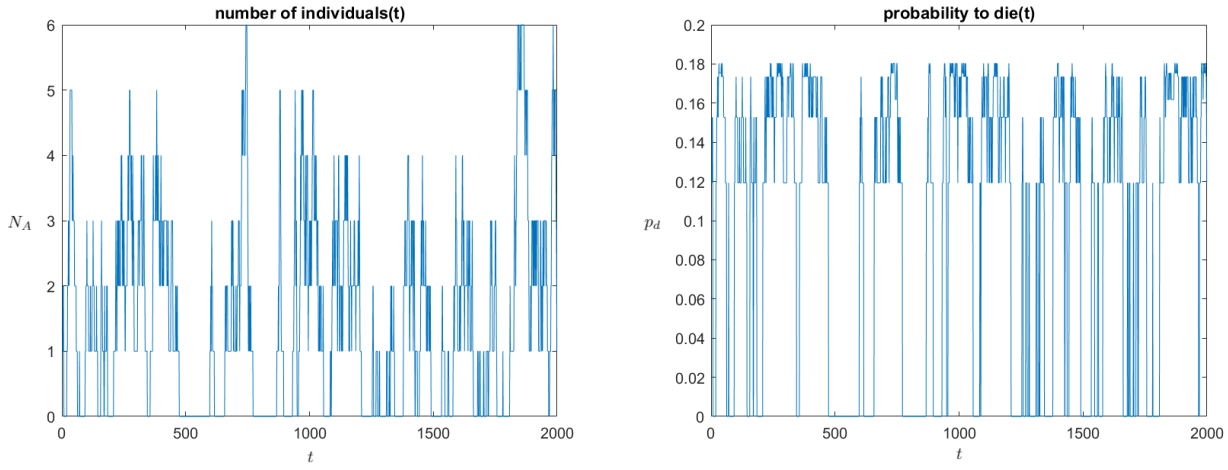

(a) (b)

Figure 15: Number of A individuals N_A and probability of an A individual to die p_d as a function of time t, from a stochastic simulation with parameters $N = 7$, $N_{A,0} = 1$, 10^5 lifetime samples taken, probability of mutation $\mu = 5\%$, $M = \begin{pmatrix} 3 & 2 \\ 5 & 1 \end{pmatrix}$ and $\beta = 1$. It is now harder to observe clear equilibrium values for both variables. However, as Tab. 5 also shows, we obtained stronger fluctuations in the death probability p_d.

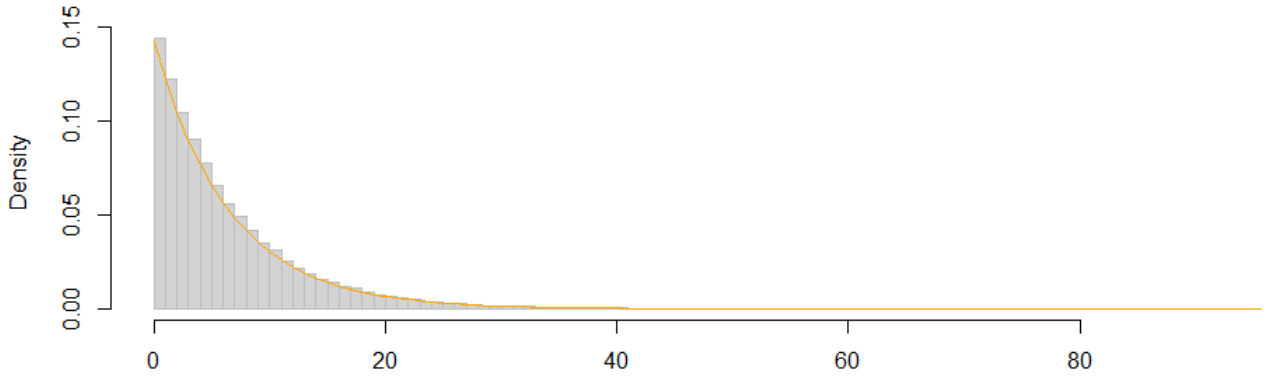

Figure 16: In grey, the normalised histogram or empiric probability density function of the simulation that yielded Fig. 15. In orange, the theoretical shape of a Geom(1/7)=Geom(1/N) distribution. Once again, we observe coincidence.

If we perform the t-test as before, this time picking the parameter $p = 1/7 = 1/N$, the result is that the mean is not $\frac{1}{p} - 1$ (with significance value $\alpha = 0.05$) for $\epsilon > 0.017$ (thus $\Delta\epsilon > 0.034$), so the tolerance is increased for $N = 7$ compared to the case $N = 100$. The tolerance is again similar to the fluctuations around the Nash equilibrium position in Tab. 5. The reason why the tolerance ϵ has increased when lowering N is that the function for the mean of the geometric distribution, $\frac{1}{p} - 1$, has more sensitivity for smaller p, or equivalently for greater N.

For the case we have just analysed (with $\beta = 1$), the number of individuals fluctuates between 0 and 6. If we wanted a stronger selection (say $\beta = 100$), so that this range is reduced (maybe to $1 - 2$) and the fluctuating values are more controlled, we have to be careful because as Tab. 6 shows, probabilities can be arbitrarily close to 0. The geometric distribution is not defined for the parameter $p = 0$, thus close values may lead to anomalies or unreliable results, Fig. 17, since lifetimes are greatly increased but simulation run time may be not so long.

position i	p_d
1	0.119266
2	0.152755
3	0.173477
4	0.180363
5	0.175346
6	0.161772
7	0.142857

Table 5: Probabilities p_d around equilibrium position 2, for the setting associated to Fig. 8 ($\beta = 1$) but instead taking $N = 7$. More noticeable fluctuations than in Tab. 4, this time of the order of 10^{-2}. However, not even this time the fluctuations beat the geometric distribution, Fig. 16.

position i	p_d
1	9.53782e-016
2	0.261905
3	0.238095
4	0.214286
5	0.190476
6	0.166667
7	0.142857

Table 6: Probabilities p_d around equilibrium position 2, for the setup of Fig. 10 ($\beta = 100$) but instead taking $N = 7$. p_d for $i = 1$ is too close to 0, meaning that it takes too long for the simulation to get deaths of A individuals when $i = 0$, and perhaps leading to anomalies (Fig. 17).

3.2 Model including ageing

One possible starting point: We consider a case in which age only affects the probability to die (so the probability that the other player beats you). This means that $h(\tau_i, \tau_j) = h(\tau_j)$, or in other words:

$$\begin{aligned} &i \text{ reproduces with probability } p_i = g(\pi_i - \pi_j) \times h(\tau_j), \\ &j \text{ reproduces with probability } p_j = g(\pi_j - \pi_i) \times h(\tau_i). \end{aligned} \tag{19}$$

Our initial choice is

$$h(\tau) = \frac{\tau}{10 + \tau}, \tag{20}$$

Note that it holds that $h(\tau) \leq 1$ for all $\tau \geq 0$. Also, realise that h in Eq. (20) is increasing, so older individuals yield greater values of h, meaning that the probability that their opponents reproduce is greater. In other words, in this setup older individuals are more likely to die.

Taking this implementation of ageing in the model, now the probability to die is much harder to compute because each individual has a specific age, thus Eq. (16) is no longer valid.

Our simulations yield Fig. 18, which shows the lifetime distribution is not geometric. It is likely that its distribution is not one of the common ones: we should determine the expression for p_d taking ageing into account and plugging it in the geometric distribution formula.

4 Cancer modelling

Moran processes models suit in general for situations in which two distinct communities clash for dominance. A particular application is cancer modelling. Let us suggest ideas for this purpose.

Firstly, in a tumor, the number of cells is not constant along time. Tumors tend to grow because cancer cells reproduce at high rates and do not die. To take this into account in a Moran process, we should not work with the exact number of cells but with the proportion of normal vs cancer cells.

Starting with one A individual in the community, which represents a mutant cancerous cell, makes sense for the scenario of a kick-off. The payoff matrix should give advantage to cancer (A) cells, so we should choose a drag payoff matrix like $M = \begin{pmatrix} 3 & 2 \\ 2 & 1 \end{pmatrix}$.

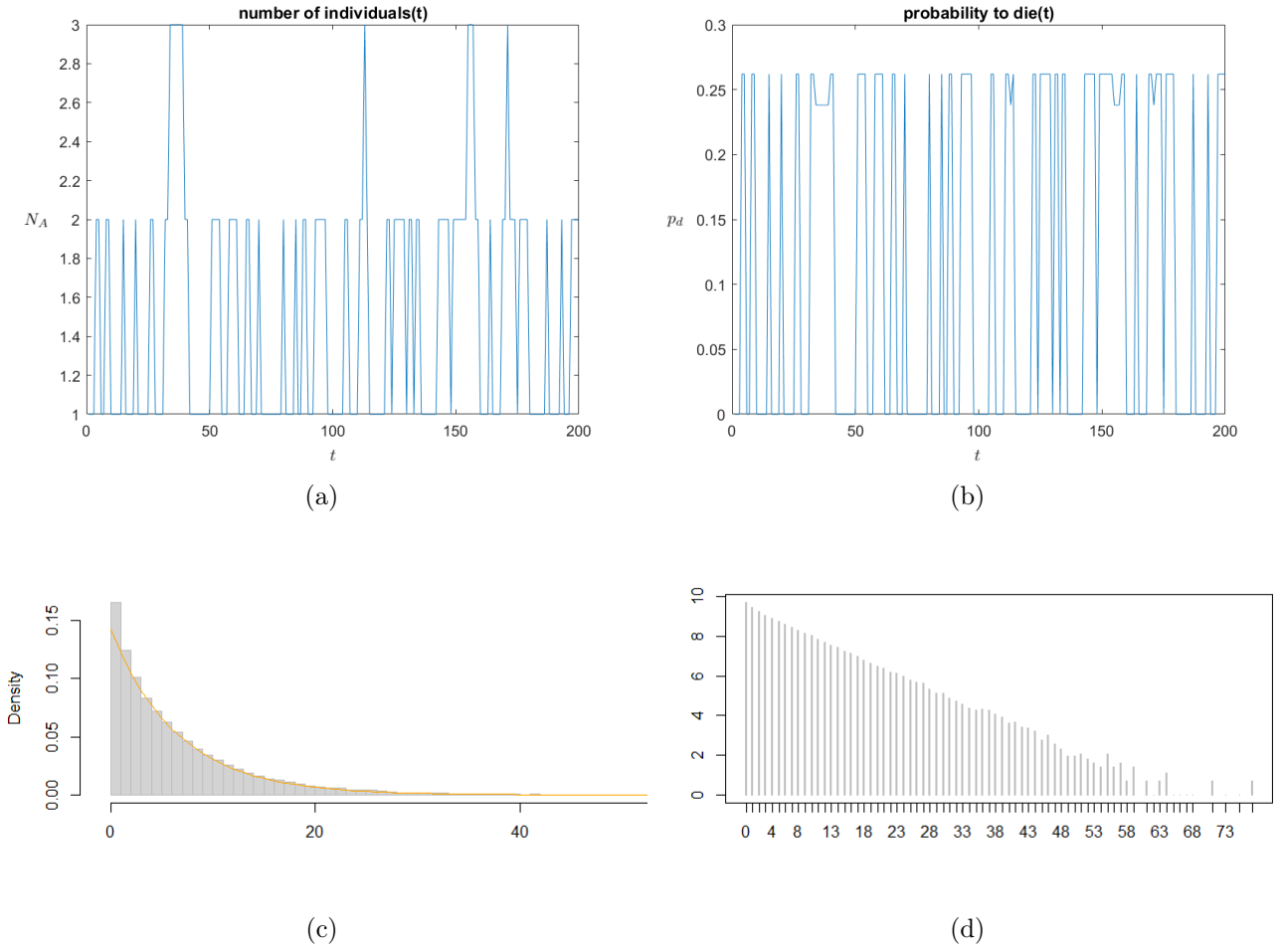

(a) (b)

(c) (d)

Figure 17: (a) Number of A individuals N_A and (b) probability of an A individual to die p_d as a function of time t, from a stochastic simulation with parameters $N = 7$, $N_{A,0} = 1$, 10^5 lifetime samples taken, probability of mutation $\mu = 5\%$, $M = \begin{pmatrix} 3 & 2 \\ 5 & 1 \end{pmatrix}$ and $\beta = 100$. (c) In grey, the normalised histogram or empiric probability density function of the simulation. In orange, the theoretical shape of a Geom(1/7)=Geom(1/N) distribution. (d) Plot of the logarithm of (c) to check linearity. There is danger of anomalies since p_d takes values too close to zero. In (c) the orange function does not fit so well this time, but this outcome is not useful to draw conclusions due to the issue about p_d.

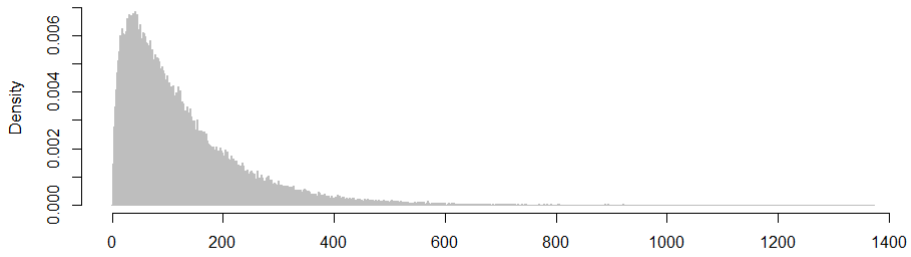

Figure 18: Empiric lifetime distribution in our model considering ageing. The setup is as in Fig. 8 (so $N = 100$ and $\beta = 1$) and we implement ageing using the ageing function of Eq. (20). Clearly not a geometric distribution, as expected, due to the ageing effect.

A realistic value for the kind of mutation we considered (A-B strategy mutation) would be $\mu = 10^{-6}$. However, we may want to take into account other types of mutation.

Definition 4.1. Driver mutations are those mutations that confer a growth advantage to cancer cells.

Definition 4.2. Passenger mutations are those mutations that do not confer a growth advantage to cancer cells.

We could forget about passenger mutations since they do not significantly affect the reproducing rates. Nevertheless, driver mutations are interesting to be included. According to the fact that they provide cancer cells with a growth advantage, we suggest to add a probability $\mu_d = 10^{-6}$ for the payoff matrix to change, for instance $M \to M + \begin{pmatrix} 2 & 1 \\ 1 & 0 \end{pmatrix}$, to strengthen the rewarding strategy A drag.

The case of human cells would not be the ideal situation to include ageing, because cancer spreads faster than cells die (human cells are replaced, on average, each 7-8 years).

Another option would be studying the treatment of cancer. One question to be answered could be: When should doctors start a treatment before chances of recovery are too low? The treatment may be implemented in the model through the payoff matrix as well, and it could depend on the proportion of cancer cells present. Consider, for example, an update of the payoff matrix for every time step like the following.

$$M(t) = M(t-1) + \begin{pmatrix} -\epsilon(a) & 0 \\ 0 & +\epsilon(a) \end{pmatrix} \tag{21}$$

a denotes the proportion of A individuals present, and ϵ is a monotonous function of a to be chosen.

As we mentioned before, it would be interesting to study how late can the treatment be provided so that the proportion of cancer cells a do not surpass a certain threshold, or so that full recovery ($a = 0$) is possible after a time.

5 Conclusions

As we have checked, Moran processes are simultaneously a relatively simple, versatile and powerful tool to study processes involving two competing communities. Simple in the sense that Fig. 2 essentially captures what a Moran process is. Versatile because it lets us include or remove features like mutation or ageing, amongst others, at our will. And powerful, taking into account that they come in handy in transcendental tasks such as cancer modelling.

This report paid special attention to the study of the lifetime distribution of individuals in a Moran process. In the lack of ageing case, we checked that the lifetime distribution follows a geometric distribution, no matter what the magnitudes of both N or β are, as justified in Section 3.1.

All in all, Moran processes unlock a vast collection of topics to explore, in many applied physics branches, such as biophysics, medicine and telecommunications.

Acknowledgments

We thank the coordinators of the SURF program, Manuel Matías and Marta, as well as Tobias's Master and PhD students, Annalisa, Fer, Rubén, and Teresa for their welcome.

This work was supported by the SURF@IFISC fellowship.

References

[1] Erwin Frey, *Evolutionary Game Theory: Theoretical Concepts and Applications to Microbial Communities*, 3-11, 2010.

[2] Philipp M Altrock and Arne Traulsen 2009 New J. Phys. 11 013012.

[3] A.F. Peralta, N. Khalil and R. Toral, *Ordering dynamics in the voter model with aging*, Physica A (2019) 122475, https://doi.org/10.1016/j.physa.2019.122475.